

Slope Pattern Spectra

I. Tchangou Toudjeu, B. J. van Wyk, M. A. van Wyk

French South African Technical Institute in Electronics
Tshwane University of Technology
ignace.tchangou@fsatie.ac.za

Abstract

In this paper, a novel algorithm using integral images, to derive *increasing slope segment pattern spectra* (called *slope pattern spectra* for convenience), is proposed. Although the proposed algorithm is not based on mathematical morphology, many pattern spectra algorithms have their roots in morphology. Granulometries based on morphological operations such as structural openings have been described for both binary and grayscale images. Pattern spectra techniques based on granulometries can be seen as global image feature extraction techniques. Many applications such as texture classification and segmentation, have proved the importance of pattern spectra for analysis and classification. The proposed *slope pattern spectra* algorithm is compared to Vincent's linear granulometric technique to approximate the depth at which laser treated High Strength Low Alloy (HSLA) steel images were taken.

1. Introduction

Traditionally, granulometries were characterized using a series of openings or closings with convex structuring elements of increasing size. Vincent, building on the work of Haralick *et al.* [14] proposed fast and efficient granulometric techniques using linear openings [7]. Granulometries, by means of their resulting pattern spectra, constitute a useful tool for texture and image analysis since they are used to characterize size distributions and shapes [10] [14].

In this paper, a novel algorithm using integral images, to derive *increasing slope segment pattern spectra* (referred to as *slope pattern spectra* in the sequel), is proposed and compared to Vincent's linear granulometric technique in terms of speed of execution and classification accuracy. The *slope pattern spectra* algorithm is not a morphological algorithm, but *similar* to morphological or linear granulometries, the proposed algorithm extracts size distributions in the form of pattern spectra.

The layout of this paper is as follows. Section 2 summarizes the concept of mathematical morphology and morphological granulometries. This section also introduces the linear granulometries proposed by Vincent [7].

The proposed *slope pattern spectra* algorithm is described in Section 3. The experimental setup and results are presented in Section 4. Future work and the conclusion are given in Section 5.

2. Morphological pattern spectra

Mathematical morphology is a general method for processing images based on set theory. Images are presented as a set of points or pixels on which operations such union and intersection are performed [1]. It was pioneered by Matheron [2] and Serra [3] at the *Ecole des Mines de Paris* in Fontainebleau in 1964. The first algorithms were derived for 2D binary images, but were later extended to grayscale images. A binary image is defined as a two-dimensional grayscale image that takes discrete gray values in the set $\{0,1\}$. Therefore morphological operations developed for grayscale images, are also relevant to binary images, but not necessarily vice versa. Two basic morphological operations are dilation and erosion [3].

Binary morphological operations are defined using Minkowski's formulism [4]. Let A be a binary image and B a structuring element with $\mathbf{b} \in B$. The *binary dilation* of A by B , denoted as $A \oplus B$ is defined by $A \oplus B = \bigcup_{\mathbf{b} \in B} (A + \mathbf{b})$, and the *binary erosion* of A by B denoted by $A \ominus B$, is defined by $A \ominus B = \bigcap_{\mathbf{b} \in B} (A - \mathbf{b})$ with $-\mathbf{b}$ belonging to the transpose of B .

In general, the dilation causes objects in the image to dilate or grow in size. The amount of growth is a function of the choice of the structuring element. Contrarily, erosion causes objects to shrink. The amount of growth or shrinkage is a function of the choice of the structuring element.

Grayscale operations are defined as follows: Let f be a grayscale image and B a structuring element. The grayscale dilation of f by B denoted by $\mathbf{d}_B(f)$ is defined by $\mathbf{d}_B(f) = \bigvee_{\mathbf{b} \in B} f_{-\mathbf{b}}$. The grayscale erosion of f by B , denoted by $\mathbf{e}_B(f)$ is defined as $\mathbf{e}_B(f) = \bigwedge_{\mathbf{b} \in B} f_{-\mathbf{b}}$. Using the extremum operations [5], these two operations are equivalent to $\mathbf{d}_B(f)(x) = \max_{\mathbf{b} \in B} f(x + \mathbf{b})$ and $\mathbf{e}_B(f)(x) = \min_{\mathbf{b} \in B} f(x + \mathbf{b})$, corresponding to grayscale dilation and grayscale erosion respectively.

Dilation and erosion (either binary or grayscale), are combined to derive two more advanced morphological operations called opening and closing. An opening is when erosion is performed, followed by dilation. The reverse is

referred to a closing. These operations are often referred as morphological filtering.

Consequently, a powerful tool for structural texture analysis is provided by mathematical morphology [4] [6]. One such a tool, derived from size distributions of objects in the image, is the pattern spectrum. The granulometries presented in the following sub-sections are from work done by Dougherty [8] [9], Maragos [10] and Vincent [7].

2.1. Morphological granulometries

Granulometries were invented by Matheron [2] and were originally applied to binary images [9]. They are considered as morphological filters involving sequences of opening or closing to extract global information in the image [3]. This process is comparable to a sieving process where particles are sieved through sieves of different sizes and shapes. Particles smaller than the size of the structuring element are removed. A *morphological pattern spectrum* is defined as the rate of sieving and can be seen as a unique signature of an image. The following definitions clarify the theory of granulometries and pattern spectra.

Definition 2.1 (Granulometry) A granulometry is defined as a family of image transformations $\{y_I\}$, $I \geq 0$ such that y_I is increasing, anti-extensive for $\forall I \geq 0$ and $y_I y_m = y_m y_I = y_{\max(I, m)}$ $\forall I \geq 0, m \geq 0$.

Definition 2.2 (Granulometry as proposed by Luc Vincent) Let $y = (y_I)_{I \geq 0}$ be a family of image transformations depending on a unique parameter I , $y = (y_I)_{I \geq 0}$ is a granulometry if and only if it forms a decreasing family of openings, that is: $\forall I \geq 0, y_I$ is an opening and $\forall I \geq 0, m \geq 0, I \geq m \Rightarrow y_I \leq y_m$.

Furthermore, a granulometry can be defined as a size distribution, which is a set of openings y_I , with $r \geq 0$, the scaling parameter. Using the function-set operation we can define the size distribution:

Definition 2.3 (Size distribution)

Let $F(r)$ be a measure of the image $f(p)$ e.g. volume of $f(p)$, by assuming that $f(p)$ is bounded, at $r=0$, $F(0) = \sum f(p)$ and at a larger value of r $F(r) = 0$, a size distribution denoted by $F(r)$ is defined by $F(r) = \sum f \circ rB(p)$.

Definition 2.4 (Normalized size distribution)

The normalized size distribution denoted by $N(r)$ and defined as;

$$N(r) = 1 - \frac{F(r)}{F(0)}, \quad (1)$$

is a cumulative distribution known as the granulometric size distribution of $f(p)$ with respect to the structuring element B with $F(r)$ being the volume of $f \circ rB$ and $F(0)$ the volume of original image $f(p)$.

$F(r)$ is referred to as a surface when dealing with binary images.

Size distributions can be used to generate *morphological pattern spectra* which is defined as the first derivative of the normalized size distribution.

Definition 2.5 (Pattern spectrum) Let $N'(r)$ be the first discrete derivative of the cumulative distribution function $N(r)$, the pattern spectrum denoted by $P(r)$ is the discrete density function, which is defined by;

$$\forall r > 0, P(r) = N'(r) = dN(r) = N(r+1) - N(r). \quad (2)$$

Note that the pattern spectrum defined in this section is a *morphological pattern spectrum*, since it is derived from morphological granulometries. The structuring element is chosen accordingly to the primitives or textons present in the texture image. It can be a rectangle, hexagon or a line, resulting in a rectangular, hexagonal or linear granulometry, respectively.

2.2. Linear grayscale granulometries

As described early, an opening operation with respect to the size of the structuring element removes all particles from the image that are smaller than the size and shape of the structuring element. This type of operation is extremely time consuming and therefore this morphological granulometry, also called the traditional granulometry, has not been used much in practice.

Linear grayscale granulometries has been found more useful than traditional granulometries. A line segment is used as a structuring element to derive a pattern spectrum which constitutes a characteristic of an image. This line segment can be in any direction depending on the primitive patterns in the image to be characterized. This concept of linear grayscale granulometries has been described by Vincent [7] who proposed the following definitions:

Definition 2.6 (Horizontal line segment) A horizontal line segment S , of length $l(S)$ is defined as a set of pixels

$$\{p_0, p_1, \dots, p_{n-1}\} \quad \text{such that for } 0 < i < n, \\ p_i = N_r(p_{i-1}).$$

Definition 2.7 (Horizontal maximum) A horizontal maximum segment M of length $l(M) = n$ in a grayscale

image I is the horizontal line segment $\{p_0, p_1, \dots, p_{n-1}\}$ such that:

$$\forall i, 0 < i < n, I(p_i) = I(p_0) \quad (3)$$

and

$$I(N_l(p_0)) < I(p_0), I(N_r(p_{n-1})) < I(p_0). \quad (4)$$

A linear opening, equivalent to the standard morphological opening of an image I by a structuring element B denoted by $I \circ B$, is proposed as:

Proposition 2.8 (Linear opening) Consider a horizontal maximum $M = \{p_0, p_1, \dots, p_{n-1}\}$, its length $l(M) = n$ and $p \in M$.

$$\forall k < n, (I \circ I_k)(p) = I(p) \quad (5)$$

for $k = 0$,

$$(I \circ I_n)(p) = \max\{I(N_l(p_0)), I(N_r(p_{n-1}))\}, \quad (6)$$

$$\forall k > n, (I \circ I_k)(p) < I(p) \quad (7)$$

By implication any opening of I by the line segment L_k such that $k < n$ leaves this maximum unchanged and for any $k \geq n$, any opening $I \circ I_k$ of p , with $p \in M$, is lower than in I .

Furthermore, the effect of the opening of size $l(M) = n$ on the pixels of the maximum M can be quantified. The value of each pixel p belonging to M is decreased from $I(p)$ to the maximum value of the neighborhood pixels $\max\{I(N_l(p_0)), I(N_r(p_{n-1}))\}$.

Hence, in granulometric terms, the contribution of maximum M to n -th bin of the horizontal pattern spectrum denoted $PS_h(I)$ is:

$$n \times \left[I(p) - \max\{I(N_l(p_0)), I(N_r(p_{n-1}))\} \right] \quad (8)$$

This is illustrated in Figure 1 where h_1 and h_2 correspond to $I(p)$ and $\max\{I(N_l(p_0)), I(N_r(p_{n-1}))\}$ respectively. The shaded area, of volume $(h_2 - h_1) * l(M)$, is the local contribution of the maximum M to the $l(M)^{th}$ bin of the horizontal pattern spectrum.

Algorithm [7]:

for (each maximum M of the considered line)

{

Adds contribution of this maximum to $l(M)^{th}$ bin of the pattern spectrum;

do {

let P be the plateau of the bin formed by opening of size $l(M)$ of M ;

if (P is itself a maximum)

computes its contribution to $l(M)^{th}$ bin of pattern spectrum;

}, **while** (P is no longer a maximum)

Special marker to skip over the maximal region around M as already processed;

}

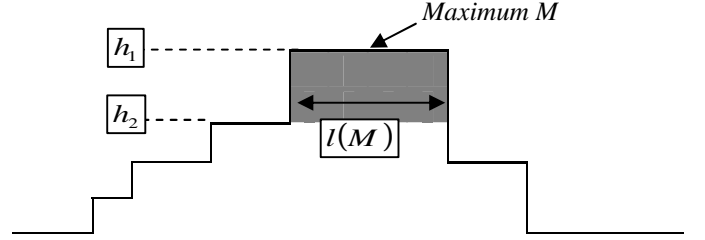


Figure 1: Cross-section of I with a maximum M .

3. The proposed algorithm for slope pattern spectrum

The *slope pattern spectra* algorithm is not a morphological algorithm, but *similar to* morphological or linear granulometries, the proposed algorithm extracts size distributions in the form of pattern spectra which in this case can be interpreted as a type of histogram. The algorithm uses an intermediate representation of the image, called the *integral image*. In this section, the proposed algorithm is described.

3.1. Basic concepts

The basic concepts required in order to understand the proposed method will first be explained. Some features referred to as “summed area tables” by Lienhard and Maydt [13], can be computed very rapidly by means of an intermediate representation of an image, termed the *integral image* by Viola and Jones [11]. The proposed algorithm also uses some aspects from the integral image concept.

Definition 3.1 (Integral image)

Let $i(x, y)$ be a grayscale image, and $ii(x, y)$ the corresponding integral image is defined as,

$$ii(x, y) = \sum_{x' \leq x, y' \leq y} i(x', y'), \quad (10)$$

computed in one pass over the original image, using

$$\begin{cases} s(x, y) = s(x, y-1) + i(x, y) \\ ii(x, y) = ii(x-1, y) + s(x, y) \end{cases}, \quad (11)$$

where $s(x, y)$ is the cumulative row and $s(x, -1) = 0$ and $ii(-1, y) = 0$.

Mitri *et al* [12] noted that the above definition can be reduced to

$$ii(x, y) = \sum_{x'=0}^x \sum_{y'=0}^y i(x', y'). \quad (12)$$

For the proposed algorithm, the integral image technique on a line segment as defined by Vincent is used. By taking a horizontal line segment S of length $l(S)$, and applying integral image transformation on it, a horizontal line segment of the same length is obtained. A formal definition for this representation is now given:

Definition 3.2 (Integral horizontal line segment)

An integral horizontal line segment S' of an grayscale image $f(p)$, of length $l(S') = n$ is a horizontal line segment $\{p_0, p_1, \dots, p_{n-1}\}$ of the integral image $F(p)$ such that

$$\text{for } 0 \leq i < n, F(p_i) = \sum_{i=0}^{n-1} f(p_i). \quad (13)$$

This is illustrated by Figure 2.

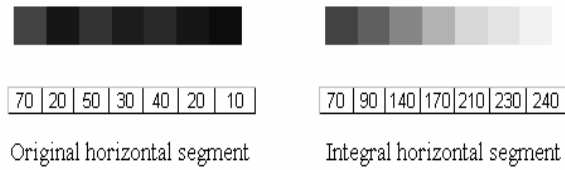


Figure 2: A horizontal line segment and its integral representation.

The right neighbor pixel is the sum of all left neighbor pixels. A growth in pixel values is observed as we move toward the right. Hence the resulting integral image is monotonically increasing from left to right.

By observing the integral horizontal line segment, a slope segment is defined as the variation in terms of intensity values when moving from one pixel location to its right neighbor. This variation can also be referred to as a discrete derivative function and expressed as

$$\forall i \in \square, \Delta F(i) = F(N_r(p_i)) - F(p_i). \quad (14)$$

The following definitions formalize these ideas:

Definition 3.3 (Slope segment) A slope segment denoted by SS , of length $l(SS) = n$ is a integral horizontal line segment $\{p_0, p_1, \dots, p_{n-1}\}$ such that

$$\forall 0 \leq i < n-1, \Delta F(i) \leq \Delta F(i+1) \quad (15)$$

or,

$$\forall 0 \leq i < n-1, \Delta F(i) \geq \Delta F(i+1) \quad (16)$$

Definition 3.4 (Increasing slope segment)

An increasing slope segment ISS , of length $l(ISS) = n$ is defined as a slope segment such that equation (15) is satisfied.

Definitions 3.2 to 3.4 are illustrated in Figure 3.

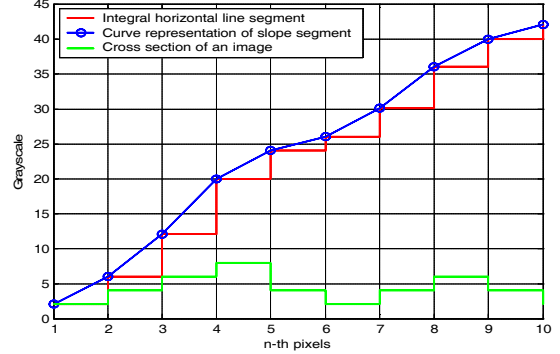


Figure 3: Illustration of a cross section of an image, its integral representation and a curve corresponding to the integral line segment indicating two increasing slope segments: The 1st one going from the 1st pixel till the 4th pixel and the 2nd one from the 5th pixel till the 8th pixel.

Slope segments compliant to Definition 3.4 are kept and the rest are discarded. Finding increasing slope segments in each horizontal line of the image can be formalized as follows: Let $m(ISS)$ be a measure of an increasing slope segment. This measure is taken as the area covered by the slope segment. In addition, we know that $ISS = \{p_0, \dots, p_{n-1}\}$ and that $\forall 0 \leq i < n-1$, $\Delta F(i) = F(N_r(p_i)) - F(p_i)$; therefore the measure of an increasing slope segment ISS is defined as

$$m(ISS) = \sum_{k=0}^{i-2} \Delta F(k) = \Delta F(p_{n-1}) - \Delta F(p_0). \quad (17)$$

and its contribution to n -th bin of the pattern spectrum is

$$\frac{m(ISS)}{n}, \quad (18)$$

where $n = l(ISS)$ is the length of the slope segment.

3.2. Increasing slope distribution

Based on the above definitions, the principle of the proposed algorithm is as follows: Consider a grayscale image $f(p)$, horizontal lines of $f(p)$ are processed one after the other, and scanned from the left to the right. Each increasing slope segment ISS , of length $l(ISS) = n$, of the horizontal line being processed is determined, its contribution to $l(ISS)^{th}$ bin of the pattern spectrum is computed and added to the current value associated with the

$l(ISS)^{th}$ bin. This operation is repeated until the last horizontal line of $f(p)$ is processed. This algorithm can be summarised as follows:

Algorithm: Pattern spectrum for a line of $f(p)$

for (each horizontal line segment of $f(p)$)

- compute the integral horizontal line segment S' ;
- **if** (S' is an increasing slope segment ISS)
 - compute and add its contribution to the current value of the $l(ISS)^{th}$ bin of the pattern spectrum;

4. Experimental setup and results

In this section we demonstrate the usefulness of the proposed algorithm by quantifying the microstructural deviation of a laser treated High-Strength Low Alloy (HSLA) from a pre-defined template. The experimental setup is first presented, followed by the results.

4.1. Experimental setup

The images of HSLA samples used for this experiment were prepared as part of a study by the *Department of Chemical and Metallurgical Engineering at Tshwane University of Technology (TUT)* to determine the effect of laser treatment on the microstructure of steel. A $1kW$ CO_2 laser with an 8 mm diameter beam was applied to HSLA samples at rate of 5 laser scan per cycles for a total of 13 cycles. At each cycle the treated sample was sectioned using a cut-off machine, mounted onto a resin, and then ground and polished using metallographic methods. At last these samples, after being etched, were viewed under a microscope with a magnification factor of 200% and then captured using a digital camera. Twenty four 256×256 images divided into groups of two, were recorded at depths of 0.2917mm , 0.5834mm , 0.8751mm , 1.1668mm , 1.4585mm , 1.7502mm , 2.0419mm , 2.3336mm , 2.6253mm , 2.9170mm , 3.2087mm and 3.5004mm . Some samples at specified depths are shown in Figure 4.

The computed slope pattern spectra of twenty four sample images from the training set (pre-defined templates) and their depth values were used to train a Generalized Regression Neural Network (GRNN) using the MATLAB neural network toolbox, to predict/estimate the depth of a test image. The GRNN is a radial function network and is a universal approximator that can solve general regression problems. It only has two layers. The first layer is constituted of a number of neurons equivalent to the number of inputs to the network and each neuron has a radial basis activation function. The second layer is the output layer. This layer has a number of neurons equal to the number of the target values and each neuron has a linear activation function. In the experiment each layer has twenty-eight neurons.

Vincent's linear horizontal pattern spectra of the HSLA test images were also computed and used in the experi-

ment, and the results compared with the proposed algorithm in terms of accuracy and speed.

4.2. Experimental results

The slope pattern spectra in Figure 4 show a good discrimination among HSLA sample images. Each pattern spectrum can be seen as a unique depth signature for each HSLA sample. As seen in Figure 4, the first and the second sample images at 0.2017 mm and 1.4585 respectively, differ in terms of their structure. These differences are reflected by their corresponding slope pattern spectra. The first slope pattern has two peaks at sizes 1 and 3, whereas the second one only has one peak at size 1. When comparing the second and the third, even the slight difference between the corresponding HSLA samples can be observed from their pattern spectra.

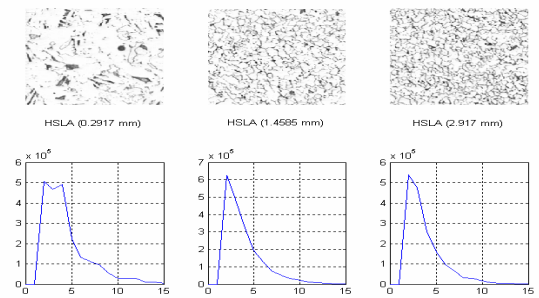


Figure 4: HSLA samples at different depth and their slope pattern spectra

Twenty four test images were collected from a sample region treated similarly and exhibiting the same microstructural properties as in the images constituting the training set. Figure 5 shows the estimated depth corresponding to each sample image of the test set. The given result was expected since some HSLA sample images are visually undistinguishable at certain depths. These results can be used to quantify the microstructural deviation between training and test images by simply calculating a similarity measure such as the mean squared error. The mean squared error of the experiment is 0.13 , which is indicative of the similarity in terms of the microstructure of the test and training sets of images. Vincent's linear granulometric algorithm, considered the most efficient granulometric algorithm, performed much worse with a mean squared error of 0.68 (Refer to Table 1).

Table 1: Accuracy in terms of mean squared error.

	Linear Algorithm	Proposed algorithm
Accuracy	0.68	0.13

Table 2: Execution time of the linear granulometry for pattern spectra shown in Figure 6, and the proposed algorithm computed for the images in Figure 4 using MATLAB and a Pentium 4 personal computer.

HSLA images	Linear Algorithm	Proposed algorithm
HSLA (0.2917mm)	145.155 s	1.406 s
HSLA (1.4585mm)	164.264 s	1.344 s
HSLA (2.9170mm)	170.327 s	1.297 s

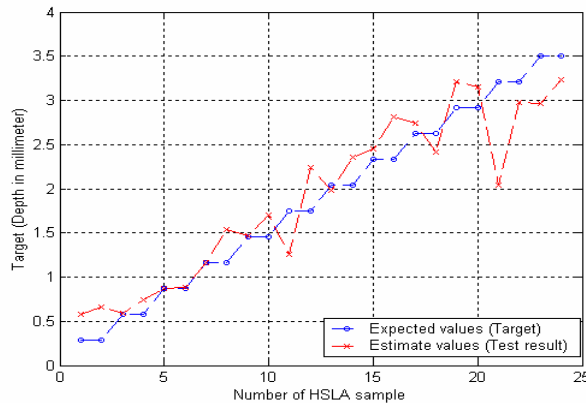


Figure 5: (-x-) is the test set result after the network has been trained and (-o-) the training set result.

Table 2 shows that the speed to compute a slope pattern spectrum is 2 orders of magnitude faster than to compute a linear pattern spectrum, referred to in the literature as a *fast algorithm*, when using MATLAB.

5. Conclusion and further works:

A novel algorithm was proposed in this paper and its application to the characterization of laser-treated HSLA samples, was presented. From the results obtained it is clear that for the specific application considered, it performed better than the linear granulometric algorithm, both in terms of accuracy and computational speed. It can be concluded that the *slope pattern spectra* is an efficient and accurate way to extract global information from a grayscale image.

Although a decreasing slope distribution was not defined in this study, future developments will explore their ability to extract global information from a given image in the form of a pattern spectrum. It will be very interesting if the slope distributions can be defined as Euclidean openings so that the proposed technique satisfies the properties of granulometries. Extensions to colour images are also under consideration.

6. Acknowledgment

The authors would like to thank the *Department of Chemical and Metallurgical Engineering at Tshwane University of Technology* for its support and especially to L.C. Kgomari for her effort in providing us with the HSLA

sample images. The NRF is thanked for supporting this work under grant TRD2005070100036.

7. References:

- [1] Bleau, J. De Guise, and A. R. Leblanc, "A new set of fast algorithms for mathematical morphology," *CVGIP Image understanding*, vol 56, no. 2, pp. 178-209, Sept. 1992.
- [2] G. Matheron, *Random Sets and Integral Geometry*, John Wiley and Sons, New York, 1975.
- [3] J. Serra, *Image Analysis and Mathematical Morphology*, Academic Press, London, 1988.
- [4] J. Serra, *Image Analysis and Mathematical Morphology*, academic Press, London, 1982.
- [5] Y. Nakagwa and A. Rosenfeld, "A note on the use of local min and max operations in digital picture processing," *IEEE Trans. Syst. Man. Cybernetics*, vol. 8, pp. 632-635. 1978.
- [6] Y. Chen and E. Dougherty, "Grayscale morphological granulometric texture classification," *Optical Engineering*, vol. 33, no. 8: pp. 2713-2722, 1994.
- [7] L. Vincent, "Fast granulometric methods for the extraction of global image information," In *Proc. PRASA*, Broederstroom, pp. 119-140.
- [8] E. R. Dougherty. "Euclidean grayscale granulometries: Representation and umbra inducement," *Journal of Mathematical Imaging and Vision*, vol. 1, no. 1, pp. 7-21, 1992.
- [9] E. R. Dougherty. *An Introduction to morphological image processing*, SPIE Tutorial Texts series, TT9, SPIE Optical Engineering Press, 1992.
- [10] P. Maragos, "Pattern spectrum and multiscale shape representation," *IEEE Transactions on Pattern Analysis and Machine intelligence*, vol. 11, pp. 701-716, 1989.
- [11] P. Viola and M. J. Jones, "Robust real-time face detection," *Internal Journal of Computer Vision*, vol. 57, no. 2, pp. 137-154.
- [12] S. Mitri, K. Pervolz, H. Surmann and A. Nuchter, "Robust object detection at region of interest with an application in ball recognition," in: *Proceedings IEEE 2005 International Conference Robotics and Automation (ICRA '05)*, pp. 126-131, Apr. 2005.
- [13] R. Lienhard and J. Maydt, "An extended set of Haar-Like feature for rapid object detection," in *Proc. ICIP '02*, pp.155-162, New York, USA, Sept 2002.
- [14] R. M. Haralick, S. Chen, and T. Kanungo. "Recursive opening transform," in *IEEE Int. Computer Vision and Pattern Recognition Conference*, Addison-Wesley, pp. 560-565, Jun. 1991.